Received 6 June 2024, accepted 29 June 2024, date of publication 11 July 2024, date of current version 15 August 2024.
Digital Object Identifier 10.1109/ACCESS.2024.3425514

RESEARCH ARTICLE

OTCFM: A Sea Surface Temperature Prediction Method Integrating Multi-Scale Periodic Features

LU-YI FAN [1], YU-HAO CAO [2], NING-YUAN HUANG [3], GUO-XUAN SUN [1], JIA-NING CAO [1], AND CHANG-XU LIU [3]
[1]Business School, Hohai University, Nanjing 211100, China
[2]School of Computer Science and Technology, Wuhan University of Science and Technology, Wuhan, Hubei 430065, China
[3]College of Computer and Information Engineering (College of Artificial Intelligene), Nanjing Tech University, Nanjing, Jiangsu 211816, China
Corresponding author: Lu-Yi Fan (lbflh5@163.com)

ABSTRACT Sea surface temperature (SST) is a critical factor in the interaction between the ocean and the atmosphere, directly influencing global climate patterns and the dynamic changes in marine ecosystems. Accurate prediction of SST is of great significance for assessing and managing global climate change and maintaining marine ecological balance. However, existing SST prediction methods face challenges such as low accuracy, short prediction periods, and significant errors. This paper proposes an innovative deep learning prediction method, Ocean Temperature Cycle Fusion and Analysis Model (OTCFM), constructed based on datasets from the South China Sea and the East China Sea. This approach aims to accurately capture and predict the cyclical variations and variability in ocean temperature data to provide more precise forecasts of ocean temperatures. Firstly, based on observations of SST's seasonal and periodic variations, we present a periodic partitioning strategy to decompose complex temperature changes into intra-period and inter-period variations. Secondly, we propose the Ocean Unit to capture both long-term and short-term small-scale changes, moving beyond the inherent attributes of the dataset's frequency and time domain characteristics to extract intra-period and inter-period feature changes simultaneously. Finally, by stacking the Ocean Units using residual connections, we alleviate the gradient vanishing problem and achieve more accurate long-term and short-term SST predictions. In this study, data from the East China Sea and the South China Sea with different spatial distribution patterns are selected for predictive analysis of the National Oceanic and Atmospheric Administration (NOAA) data from September 1, 1981, to June 7, 2023, with a total of 15,408 data. The experimental results show that OTCFM can accurately capture the evolution patterns of SST data in the spatial and temporal processes under different experimental conditions. The MAE values on the East China Sea and South China Sea SST datasets are improved by 19.08% and 19.52%, respectively, compared with the convolutional long short-term memory neural network (ConvLSTM), which improves the accuracy of the long and short-term prediction of SST time series and has a far-reaching impact on the subsequent promotion of sustainable marine resource management and environmental protection.

INDEX TERMS Sea surface temperature, time series prediction, periodic partitioning, adaptive fusion.

I. INTRODUCTION

The oceans cover 70% of the Earth's surface, and their variability profoundly affects the global climate. Sea surface temperature (SST) is a central indicator of ocean thermal energy, which reflects the energy exchange in the global atmospheric and marine ecosystems and dramatically impacts many climate and environmental issues, such as ocean acidification, rainfall distribution, and typhoon formation [1]. It reflects the energy exchange in the global atmospheric and oceanic ecosystems and greatly influences many climate and environmental issues, such as ocean acidification,

The associate editor coordinating the review of this manuscript and approving it for publication was Tao Wang.

rainfall distribution, and typhoon formation. Therefore, accurate prediction of the SST evolution pattern is meaningful for many environment-related research activities. However, the complexity of the marine environment and the many factors that influence the accurate prediction of SST are challenging in time and space [2].

At the same time, with the increase of human activities at sea, the increased reliance on marine resources also implies higher requirements for predictive analysis of marine environmental elements, such as the rapid development of space launch activities at sea in recent years, which puts forward a higher demand for the observation of many marine elements [3]. However, current prediction techniques are still unable to meet the demand for long-term stable operation and more accurate predictions of over-water systems. Specific challenges in the existing prediction tasks include: (1) SST exhibits significant seasonal and cyclic variations, e.g., atmospheric conditions and tropical currents directly or indirectly affecting SST. Only multi-step temporal projections can track the evolution of SST over long time scales. (2) Existing ocean prediction tasks are limited to the extraction of intrinsic attributes such as frequency domain features and time domain features of the dataset itself, ignoring short-term, small-amplitude variations in the sea surface temperature time series, including intermixing and overlapping variations of rising, falling, and fluctuating sea surface temperatures, all of which make the process of modeling the time series of sea surface temperatures more challenging.

The currently available sea surface temperature prediction methods can be categorized into two main groups. One is numerical methods, and the other is data-driven methods. Numerical methods are based on physical, chemical, and biological parameters and their complex interactions. They describe the relationship between sea surface temperature changes by establishing a series of mathematical-physical equations to build corresponding mathematical prediction models. Richter et al. used linear inverse models (LIMs) and atmospheric circulation models to make statistical forecasts of tropical Sea Surface Temperature using linear inverse models (LIMs) and atmospheric circulation models [4]. Yati et al. effectively predicted and assessed the change of SST in the North Pacific Ocean using 23 years of data from the Copernicus Climate Change Service Center [5]. However, numerical modeling is limited by the high complexity of the physical equations and the sizeable computational volume, suppressing the time series performance. It is more suitable for predicting SST at large scales with relatively low resolution while requiring higher conditions for hardware equipment, and it isn't easy to simulate nonlinear sequences [6].

On the other hand, data-driven methods learn patterns of SST variability from historical data to model sea surface temperature prediction. Compared to numerical methods, they require less knowledge of the marine and environmental domains. They can predict sea surface temperatures at a high resolution on more minor scales, with efficient fitting of nonlinear relationships, and do not require much hardware equipment. Traditional data-driven methods are available in several forms, such as logistic regression, decision trees, and artificial neural networks. For small-scale data, these methods can obtain more accurate prediction results [7]. However, traditional machine learning algorithms have many shortcomings when faced with large-scale sea temperature data, especially temperature data with long time spans and drastic changes [8], [9].

With the development of deep learning technology, it has been widely used as an end-to-end computational method in the fields of climate research [10], satellite remote sensing [11], and power systems [12]. A recurrent neural network (RNN) is a class of neural networks that can store memory, and the gradient disappears when dealing with long time series [13]. Long-short-term memory (LSTM) [14] is an improved RNN capable of learning long-term dependent information in a time series through a specific gate structure mechanism to prevent back propagation errors. Gated Recurrent Unit (GRU) [14] builds on LSTM by retaining only the update and reset gates, mitigating the overfitting and underfitting phenomena that may occur with training. The three deep learning methods have all achieved better prediction performance in SST forecasting [15].

Based on the above deep learning methods, Liu et al. [16] were the first to employ convolutional neural networks (CNNs) to extract relevant features from historical ocean temperature and salinity data. The extracted vital features were input into an LSTM network for SST prediction. Zhang et al. [17] developed a mid-to-long-term SST prediction model based on the GRU neural network algorithm. This model utilized monthly and quarterly SST data, selecting the Bohai Sea area, which exhibits significant annual temperature variations, for its predictions. The GRU layers captured the temporal relationships inherent in the SST data. It is important to note that while single deep learning models are adept at capturing subtle changes between consecutive time points in time series data, they often struggle to simultaneously identify spatial and temporal dependencies when dealing with data features spanning different periods.

Researchers have used the attention mechanism and its variants in sea surface temperature prediction tasks in recent years, combining them with other deep learning methods. Lin et al. [18] further improved the prediction results by integrating the self-attention mechanism with LSTM for sea surface temperature prediction. However, it is difficult for the attention mechanism to find reliable dependencies directly from dispersed time points. Data dependencies between neighboring periods may be ignored and blurred in the complex time series feature extraction process [19].

To adapt to the complex and changing marine environment, this paper analyzes the time series from the perspective of multiple cycles. First, we observe that the time series of sea surface temperature is usually affected by weeks, months, and quarters, showing multi-periodicity, while multiple cycles cross and interact with each other, making it relatively complicated to model based on historical sea surface temperature. Secondly, considering that the sea surface temperature series data between neighboring periods are interdependent during data acquisition, it is difficult for past deep learning methods to capture the data dependencies located at neighboring time points within a cycle. Based on this, in this paper, the sea surface temperature data trends are further categorized into inter-period variation and intra-period variation. Inter-week variability reflects the long-term trend of sea surface temperature changes with periods such as year, quarter, month, etc. In contrast, intra-period variability implies a small range of short-term variability characteristics within a certain period.

In this paper, to further capture the intra-periodic and inter-periodic features in the SST time series, we propose an advanced deep learning method, the Ocean Temperature Cycle Fusion Model (OTCFM). This method extracts features from the re-divided two-dimensional time-series matrices through a modular approach called Ocean Unit. The inter-periodic feature extraction module utilizes autocorrelation coefficients (ACCs) to determine convolution kernel sizes, aiming to mine the short-term strong correlations in the time series data. By applying weight sharing, the method also avoids the problem of parameter explosion. To ensure that the subtle changes of the close neighboring time points within a specific period can be captured, the intra-period feature extraction module uses a multi-layer structure of MLP for smooth feature extraction. Finally, based on the weighted aggregation of amplitudes, a feature that integrates many different frequencies and intra-periodic and inter-periodic features is obtained, providing a new method for analyzing and predicting SST data.

In addition, two sea areas with different spatial distribution patterns, the East China Sea and the South China Sea, are used as the study areas in this paper to implement a comprehensive prediction task for the surface temperatures of the selected sea areas. The main contributions of this paper can be summarized as follows:

(1) We used the Fast Fourier Transform to spectrally analyze the sea surface temperature series, reclassifying and obtaining the different cycles that contain the maximum information and maximally preserving the two different types of local characteristics of the time-series data.

(2) To accomplish high-precision long- and short-term SST time prediction, We implement intra-period and inter-period feature extraction by Ocean Unit, a modular modeling method proposed in this paper.

(3) Based on the complex interactions between intra-periodic and inter-weekly periods of the SST time series, we propose a deep learning method, OTCFM, oriented to SST prediction to capture the long- and short-term variations of the SST and predict the state and trend in the future period by connecting Ocean Unit in a residual stacking manner.

(4) A comprehensive comparative analysis with classical and state-of-the-art baseline methods is conducted, and the experimental results demonstrate the superiority of our proposed deep learning method, OTCFM, in SST time series prediction.

The rest of the paper is organized as follows: Section II defines the problem for sea surface temperature prediction. Section III presents the details of the OTCFM proposed in this paper. In Section IV, we conduct a series of experiments to demonstrate the effectiveness and superiority of our proposed method. Finally, we provide a comprehensive summary of the paper.

II. PROBLEM DEFINITION

The ocean surface temperature is usually divided into a grid system according to latitude and longitude, forming a height and width temperature matrix W to record temperature data at a specific point in time $T(i)$. Here W, the number of grids along the latitude and longitude directions is represented. The temperature matrix forms a sequence over time that records historical changes in ocean surface temperature. Formally, given a historical sea surface temperature series $([T_1, T_2, \ldots, T_m])$ with time step m, the objective is to predict the sea surface temperature series $([T_{m+1}, T_{m+2}, \ldots, T_{m+n}])$ with step n, and the prediction process can be expressed as:

$$T_{m+1}, T_{m+2}, \ldots, T_{m+n} = \zeta([T_1, T_2, \ldots, T_m]) \tag{1}$$

where ζ denotes a segment mapping.

III. METHODOLOGY

A. OVERVIEW

In this paper, to accurately capture and predict the cyclical changes and variability of ocean temperature data, we propose for the first time a state-of-the-art deep learning method for SST prediction scenarios, namely OTCFM. Figure 1 illustrates the model structure of the proposed OTCFM. The overall structure is formed by stacking Ocean Unit components through complete connections. Ocean Unit first utilizes the Fast Fourier Transform method to divide adequate periods. Then, it uses an efficient feature extraction module to capture time-varying features within and between periods, finally integrating and outputting the results. In the inter-period feature extraction module, inspired by convolutional neural networks, convolutional kernels capture the time correlations between time series values of different periods. Meanwhile, we use the autocorrelation coefficient (ACC) calculation to determine the size of the convolutional kernels, aiming to achieve higher feature extraction capabilities. In the intra-period feature extraction module, we choose the multi-layer perceptron (MLP) as the relevant extraction component, using a multi-layer structure to achieve smooth feature extraction and capture subtle changes within specific periods as much as possible.

1) PERIOD SEGMENTATION MODULE

Without the aid of other external attributes, when only using the SST time series within a period in the past for temperature prediction, it is easy to neglect the long-term temporal trend and only focus on the temperature change relationship in

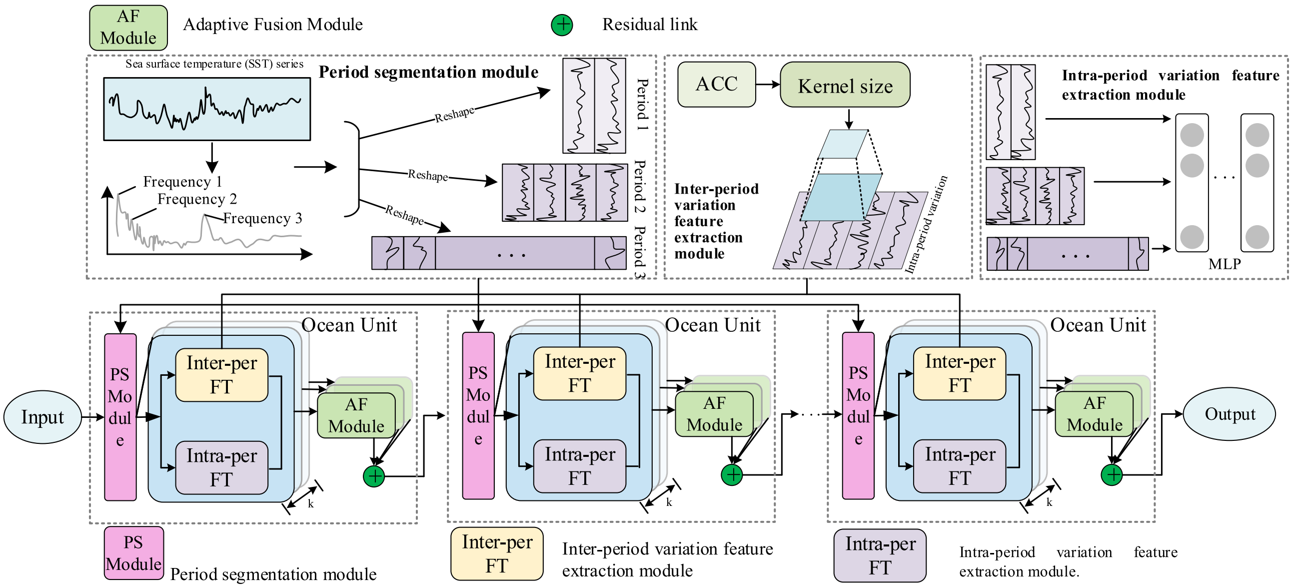

FIGURE 1. Overview of the proposed OTCFM.

the neighboring time points. Therefore, to take into account both intra-periodic and inter-periodic temperature trends, the period of the sea surface temperature series will be further redefined and divided in this paper to overcome the limitations brought by the original one-dimensional series.

Specifically, the Fast Fourier Transform used can visually identify the period and frequency of the central time series through spectral analysis and complete the conversion of frequency domain data. In this paper, we use $FFT(\cdot)$ it to denote the Fourier transform that the temperature time series undergoes $Amp(\cdot)$ to obtain the amplitude of the Fourier transform resultant image and $Avg(\cdot)$ to find the mean value. We can write the transformation process as follows:

$$\mathrm{V} = Avg(Amp(FFT(T_{\mathbf{1D}}))) \tag{2}$$

Many signals concentrate their energy in a few frequency components in the frequency domain. In contrast, the energy distribution at other frequencies is tiny. The spectrum obtained from the Fourier transform of the SST time series data can contain the amplitude values of each frequency component. To highlight the significant frequency components, we focus only on the k frequency components with the largest amplitudes and ignore the rest of the smaller components. Equation (3) shows the overall process.

$$\begin{aligned} \{\mu_1, \cdots, \mu_z\} &= \arg Topk(\mathrm{V}), \\ &\times \mu_* \in \left\{1, \ldots, [\frac{M}{2}]\right\}, z \in \{1, \cdots, k\} \end{aligned} \tag{3}$$

where $\{\mu_1, \cdots, \mu_z\}$ denotes the most significant frequency chosen, where k is the hyper-parameter. Due to conjugate symmetry, only the positive frequency part, i.e. $\mu_* \in \left\{1, \ldots, [\frac{M}{2}]\right\}$, is retained in the calculation. Based on the given frequencies μ_{f_i} and the time series length M, the cycle length p_z

$$p_z = \frac{M}{\mu_z}, z \in \{1, \cdots, k\} \tag{4}$$

Thus, we can further write equation (1) as:

$$\mathrm{V}, \{\mu_1, \cdots, \mu_z\}, \{p_1, \ldots, p_z\} = Per(T_{1D}) \tag{5}$$

The 1-dim time series is re-modeled according to the reclassified period $\{p_1, \ldots, p_z\}$ using the 2-dim matrix, and the temperature time series data is shape-padded $Padding(\cdot)$ as follows:

$$T_{\mathrm{2D}}^{z} = \mathrm{Reshape}_{p_z, \mu_z}\left(\mathrm{Padding}(T_{\mathrm{1D}})\right), z \in \{1, \cdots, k\} \tag{6}$$

where and constrain the shape of the formed 2-Dim matrix, i.e., the rows and columns, which can also reflect the temporal trends within and between cycles corresponding to the selected cycle lengths. After a series of transformations, a set of 2-Dim matrices $\{T_{2D}^1, \ldots, T_{2D}^k\}$ derived from different cycles is finally obtained, which contains two different types of local properties at the same time:(a) Within the same cycle, the time points corresponding to neighboring columns of the matrix are adjacent to each other, implying changes within the cycle of the temperature series. (b) For moments located within different cycles, adjacent rows of the matrix correspond to contiguous cycles, and obtaining features from the direction of the row projections better captures the trend of the temperature series from cycle to cycle.

2) OCEAN UNIT

Given an SST time series $([T_1, T_2, \ldots, T_m])$ of length m, reclassified and modeled by the period extraction module to obtain $\{T_{2D}^1, \ldots, T_{2D}^k\}$ further capture of inter-period variation and intra-period variation features, we design two modules to perform feature extraction separately.

a: INTER-PERIOD VARIATION FEATURE EXTRACTION MODULE

Convolutional Neural Networks (CNN) have powerful image-processing capabilities and can simultaneously process tens of millions of image values. We can consider the transformed 2-Dim tensor as an image pixel point and perform image-like feature extraction operations. We will design the local sensing field mechanism of CNN to sense the pixel points locally in close neighboring neighborhoods, which can reduce the network's parameters while mining the temporal data for short-term solid correlations. The size of the convolutional kernel determines the size of the receptive field. The size of the receptive field is determined by the convolutional kernel size $I_1^{C(l)} \times I_2^{C(l)}$, which also determines the mapped range of the output feature values of each layer. We can formalize the convolution process by transforming the time series cycles according to their division:

$$\hat{T}_{2D}^{z} = kernel_{I_1^{C(l)} \times I_2^{C(l)}}(T_{2D}^{z}),\ z \in \{1, \cdots, k\} \tag{7}$$

To obtain inter-period variation characteristics, when the column size $I_2^{C(l)}$ of the fixed convolution kernel is C, convolution kernels with different row sizes $I_1^{C(l)}$ have varying weights in capturing periodic characteristics. We can effectively determine the convolution kernel size by calculating the ACC of the sea surface temperature time series over periods. The autocorrelation coefficient, which represents the lag i order of the time series, can be expressed as follows:

$$\gamma_i^{acc} = \frac{\mathrm{V}(t(x), t(x-i))}{\sqrt{\mathrm{V}(t(x))\mathrm{V}(t(x-i))}}, \tag{8}$$

where V denotes the variance, and ACC represents the linear correlation between measurement points separated by i intervals. Notably, the correlation among column elements represents the correlation within a period, while the correlation among row elements represents the inter-period correlation. Accordingly, the row size $I_1^{C(l)}$ of the convolution kernel is determined by the inter-period correlation, while the column size $I_2^{C(l)}$ of the convolution kernel depends on the intra-period correlation. Thus, the row size $I_1^{C(l)}$ of the convolution kernel can be determined as follows:

$$\begin{aligned} I_1^{C(1)} &:= \{j \mid j \geq 1 : \gamma_{j*p+1}^{acc} > \gamma\}, \\ I_2^{C(1)} &:= C, \end{aligned} \tag{9}$$

where γ is a pre-set threshold value, in this paper, set. $\gamma = 0.5$

After applying the convolution kernel transformation, the 2-D matrix $\hat{T}_{2D}^{z}$ is truncated and restored to its original sequence length M. The digital form of this process is represented as follows:

$$\hat{T}_{In-ID}^{l,i} = \mathrm{Reshape}_{1,(p_i \times f_i)}\left(\hat{T}_{2D}^{l,i}\right),\ i \in \{1, \cdots, k\} \tag{10}$$

Additionally, thanks to the periodic extraction module, we have accomplished the multi-period division of the one-dimensional raw sequence. On this basis, convolution kernels determined by the autocorrelation coefficient can capture the periodic variations in the sea surface temperature sequence, thereby uncovering the temporal correlations between time series values within different periods. Moreover, the short-term strong correlation of the time series allows us to avoid issues such as parameter explosion by applying the weight-sharing method.

b: INTRA-PERIOD VARIATION FEATURE EXTRACTION MODULE

To enhance the extraction of intra-period features in sea surface temperature, we selected the MLP component as the optimal solution. The MLP can achieve smooth feature extraction through a multi-layer structure, capturing subtle changes within specific periods in time series data as much as possible. The MLP has multiple neurons, each connected to all neurons in the previous layer. By adjusting the values of elements in the weight matrix, the correlation within each column vector, i.e., the intra-period temporal dependency relationship, can be obtained, as shown in the formula.

$$\hat{T}_{\text{Between-ID}}^{l,i} = Relu(W_l T_{2D}^{z} + b_l) \tag{11}$$

where l denotes the depth of the feedforward neural network and b_l each layer's bias. The ReLU is capable of performing nonlinear transformations to capture more complex patterns.

c: ADAPTIVE FUSION MODULE

For the generated k-periodic features $\{\hat{T}_{in-ID}^{l,1}, \ldots, \hat{T}_{in-ID}^{l,k}, \hat{T}_{Between-ID}^{l,1}, \ldots, \hat{T}_{Between-ID}^{l,k}, \}$, we observe that the amplitude A can be used to measure the importance of each transformed one-dimensional representation in the overall feature extraction, where we will use amplitude-based weighted aggregation to obtain a feature that combines several different frequencies as well as intra- and inter-periodic periods.

$$\begin{aligned} &\hat{T}_{f_1}^{l-1}, \cdots, \hat{T}_{f_k}^{l-1} \\ &\quad = \mathrm{Softmax}\begin{pmatrix} \hat{T}_{\text{in-ID}}^{l,1}, \ldots, \hat{T}_{\text{in-ID}}^{l,k}, \\ \hat{T}_{\text{Belween-ID}}^{l,}, \ldots, \hat{T}_{\text{Between-ID}} \end{pmatrix} \\ &\hat{T}_{\text{ID}}^{l} = \sum_{i=1}^{k} \hat{\mathbf{A}}_{f_i}^{l-1} \times \hat{T}_{\text{ID}}^{l,i}. \end{aligned} \tag{12}$$

It is worth noting that the components mentioned above, including the period segmentation module and the feature extraction modules within and between periods, together constitute the Ocean Unit. To predict sea surface temperature more accurately over a future period, we stack the Ocean Unit using a residual network approach. By incorporating skip connections, we ensure smoother information flow between Ocean Units, addressing the issues of gradient vanishing and exploding in the SST time series prediction task and significantly enhancing prediction performance. The process is formalized as follows:

$$T_{\text{ID}}^{l} = \mathrm{OceanUnit}\left(T_{\text{ID}}^{l-1}\right) + T_{\text{ID}}^{l-1}. \tag{13}$$

In the entire SST prediction process, we have redefined and interpreted periodicity, reshaped the dimensions of the time series, and overcome the limitations of the original one-dimensional spatial vector representation. This approach retains all intra-period and inter-period features, and the adaptive fusion module balances long-term and short-term prediction performance, demonstrating a solid feature extraction capability. The proposed OTCFM method achieves good SST time series prediction task results. Section IV provides detailed empirical evaluations and discussions.

B. PREPARATION

(1) Data Selection. Similar to many literatures that use deep learning methods for sea surface temperature prediction, the experimental data in this paper is the best-interpolated SST data (daily OISST, version 2) produced by the National Oceanic and Atmospheric Administration (NOAA) Data Center. This dataset contains daily mean SST observations on a global scale, with a spatial resolution of 0.25°x0.25°, and spans the period from September 1, 1981, to June 7, 2023, with a total of 15,408 data entries. The dataset provides a complete ocean temperature field with high temporal and spatial coverage by combining bias-adjusted observations from different digital acquisition platforms (e.g., satellites, buoys) on a global latitude-longitude grid.

(2) Region Selection. To maximize the exploration of the application effect of our proposed method in different sea areas, we selected the South China Sea, where the change of sea characteristics is gentler, and the East China Sea, where the change is more significant, as the study areas in this study, while avoiding land areas as much as possible. Expressly, the study area of the South China Sea is set between 14.125° and 20.125° N latitude and 110.625° and 116.625° E longitude, covering 24×24 grid points. In comparison, we set the study area of the East China Sea between 26.875° and 32.875° N latitude and 121.375° and 127.375° E longitude, including 24×24 grid points.

(3) Dataset division. To answer the research questions posed above, the entire OISST dataset was further divided for training, validation, and testing, where 70% of the data from September 1, 1981, to September 1, 2022, was used for training and 30% for validation, and the data from September 1, 2022, to June 7, 2023, was used as the test dataset. Specifically, the training dataset contains 15,129 samples, and the test dataset includes 279 samples.

To accelerate the training speed of the model, in this paper, the maximum and minimum normalization is applied to the SST training set to normalize the data to [0,1] with the following formula:

$$x^* = \frac{x - x_{\min}}{x_{\max} - x_{\min}} \tag{14}$$

where x^* denotes the normalized SST, x denotes the actual observed SST, $x_{\min}$ denotes the minimum value of the actual observed SST, and $x_{\max}$ denotes the maximum value of the actual observed SST.

(4) Evaluation Metrics. In the context of the SST time series prediction task, this paper employs four widely used evaluation metrics: Root Mean Square Error (RMSE), Coefficient of Determination (R^2), Mean Absolute Error (MAE), and Mean Absolute Percentage Error (MAPE) to assess the accuracy of our proposed method. The specific definitions are as follows:

$$RMSE = \sqrt{\frac{1}{n}\sum_{i=1}^{n}\left(\hat{y}_i - y_i\right)^2} \tag{15}$$

$$R^2 = 1 - \frac{\sum_{i=1}^{n}\left(\hat{y}_i - y_i\right)^2}{\sum_{i=1}^{n}\left(\bar{y}_i - y_i\right)^2} \tag{16}$$

$$MAE = \frac{1}{n}\sum_{i=1}^{n}\left|\hat{y}_i - y_i\right| \tag{17}$$

$$\text{MAPE} = \frac{100\%}{n}\sum_{i=1}^{n}\left|\frac{y_i - \hat{y}_i}{y_i}\right| \tag{18}$$

where $\hat{y}$ represents the predicted value of SST, y represents the actual observed value of SST, $\bar{y}$ represents the average value of the actual observation, and the smaller the value of MAE and RMSE, the better the prediction performance of the algorithm.

(5) Equipment parameters. The proposed algorithm's experimental design and baseline model were executed on a hardware configuration of a 64-bit Windows server equipped with an Intel Core i9-13900HX processor, GeForce RTX 4060 graphics card, and a 3TB hard disk. The Win 11 operating system is the software environment, and the integrated development environment is selected as VSCODE.

IV. EXPERIMENTS

To validate the prediction performance of our proposed OTCFM, this section conducts comprehensive experiments on real marine datasets to answer the following research questions (RQs):

RQ1: Does our proposed OTCFM outperform the classical baseline methods of the past and the current state-of-the-art forecasting methods?

RQ2: Can the OTCFM perform long-term sea surface temperature forecasts effectively?

RQ3: How do the intra-periodic and inter-periodic feature extraction modules affect the prediction accuracy of OTCFM?

RQ4: How do the visualization results of the proposed OTCFM perform?

A. COMPARISON OF PREDICTION PERFORMANCE WITH OTHER MODELS(RQ1)

To evaluate the effectiveness of our proposed OTCFM, we compared it with four classic methods, including three baseline models: LSTM [20], TCN [21], ConvLSTM [22], and an advanced model 3D U-Net [23].

TABLE 1. SST prediction performance of OTCFM and baseline models on south china sea and east china sea datasets.

		South China Sea				East China Sea			
Metric	Method	1d	2d	3d	4d	1d	2d	3d	4d
	LSTM	0.482	0.499	0.531	0.671	0.525	0.534	0.581	0.611
	TCN	0.491	0.502	0.566	0.621	0.491	0.511	0.542	0.602
	ConvLSTM	0.397	0.406	0.511	0.598	0.457	0.501	0.514	0.527
	3D U-Net	0.308	0.372	0.411	0.459	0.422	0.451	0.467	0.481
RMSE	OTCFM	0.221	0.261	0.302	0.386	0.311	0.324	0.335	0.341
	LSTM	0.939	0.931	0.922	0.901	0.925	0.911	0.909	0.899
	TCN	0.941	0.933	0.921	0.911	0.937	0.929	0.921	0.916
	ConvLSTM	0.957	0.948	0.931	0.922	0.949	0.941	0.936	0.928
	3D U-Net	0.961	0.952	0.944	0.931	0.957	0.949	0.937	0.926
R2	OTCFM	0.991	0.982	0.979	0.961	0.986	0.977	0.969	0.958
	LSTM	0.361	0.377	0.411	0.438	0.379	0.382	0.391	0.402
	TCN	0.355	0.382	0.396	0.427	0.366	0.371	0.382	0.391
	ConvLSTM	0.344	0.352	0.361	0.392	0.353	0.361	0.375	0.382
	3D U-Net	0.327	0.345	0.351	0.381	0.331	0.342	0.351	0.361
MAE	OTCFM	0.291	0.305	0.311	0.327	0.318	0.326	0.334	0.351
	LSTM	1.37%	1.44%	1.52%	1.67%	1.47%	1.55%	1.61%	1.72%
	TCN	1.29%	1.35%	1.44%	1.59%	1.35%	1.41%	1.52%	1.62%
	ConvLSTM	1.01%	1.14%	1.22%	1.31%	1.18%	1.27%	1.34%	1.41%
	3D U-Net	0.97%	1.02%	1.11%	1.29%	1.02%	1.12%	1.21%	1.31%
MAPE	OTCFM	0.75%	0.81%	0.88%	0.94%	0.81%	0.87%	0.97%	1.04%

1) LONG SHORT-TERM MEMORY NETWORK (LSTM)

LSTM features a unique gating mechanism that can better capture long-term dependencies in sequential data, learning patterns, and features in time series data.

2) TEMPORAL CONVOLUTIONAL NETWORK (TCN)

The TCN model has higher parallelism and a more flexible receptive field, saving significant runtime.

3) CONVOLUTIONAL LSTM NETWORK (CONVLSTM)

The ConvLSTM model establishes temporal relationships similar to LSTM and possesses spatial feature extraction capabilities akin to CNN.

4) 3D U-NET

The 3D U-Net model can utilize a three-dimensional U-Net structure combined with multi-source sea surface variables to predict sea temperature, playing different roles in various prediction periods.

To evaluate the effectiveness and feasibility of the OTCFM method in sea surface temperature forecasting, we conducted a detailed comparison with four other methods. In the SST forecasting task, the prediction step directly affects the forecasting results. Generally, as the prediction step increases, the forecasting accuracy decreases. Considering that the prediction step is closely related to ocean forecasting and prediction systems, we conducted experiments on sea temperature datasets from the South China Sea and the East China Sea, fixing the prediction steps at 1 day, 2 day, 3 day, and 4 day. The results are shown in Table 1.

Table 1 shows that in the short-term prediction process, since the LSTM model only extracts the time-dependent features of the SST data without considering the spatial features, the prediction accuracy is the worst, with a prediction RMSE of 0.482 at 1 day. Due to the insufficient extraction of spatial features, the performance of the ConvLSTM model is worse, with an RMSE of 0.397. In contrast, our proposed Ocean Unit model shows significant advantages. It effectively captures the multi-periodic features, and the 2D vectors generated by feature transformation are highly structured and rich in information. The columns and rows of these vectors represent the positional relationships between time points and periods, respectively. The OTCFM model performs optimally in all four evaluation metrics by adequately modeling the cyclic patterns.

Specifically for the 4 d prediction task, the OTCFM model achieves MAE, RMSE, and MAPE of 0.327, 0.386, and 0.94%, respectively, better than the TCN model's 0.427, 0.621, and 1.59%. Despite the advantages of the TCN model in parallel computation and handling sequences of different lengths, it is still insufficient in capturing the long-term time dependence, which further emphasizes the advantages of the OTCFM method. On the 4 day, the MAE, RMSE, and MAPE of the ConvLSTM model were 0.392, 0.511, and 1.31%, respectively. Although the ConvLSTM model can capture the spatial distribution features, its prediction accuracy is still limited when dealing with complex and variable temperature information, making it challenging to meet the demand for accurate prediction.

In addition, we find that although 3D U-Net shows good prediction performance in predicting the surface temperature of the South China Sea with MAE, RMSE, and MAPE of 0.381, 0.459, and 1.29%, respectively, it performs poorly in predicting the temperature of the East China Sea. This difference may be because the South China Sea is relatively far from the mainland, less affected by human activities, more direct environmental factors, and less interference in the prediction process [24].

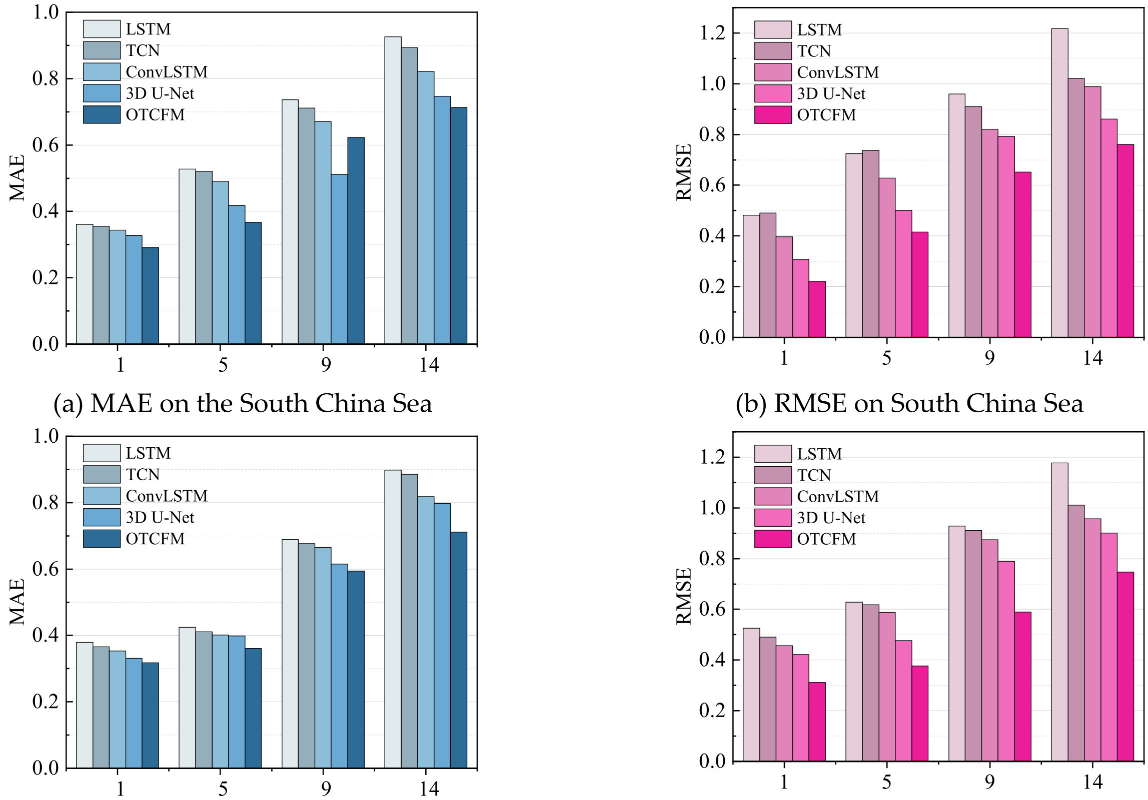

(a) MAE on the South China Sea (b) RMSE on South China Sea

(c) MAE on the East China Sea (d) RMSE on the East China Sea

FIGURE 2. **Comparison of medium and long-term prediction errors of different models on the East and South China Sea test sets.**

B. MEDIUM TO LONG-TERM SST PREDICTION(RQ2)

The prediction of SST in the medium to long term can provide early warnings of temperature changes over extended periods. This information is valuable for industries such as fisheries and shipping, which rely on ocean conditions. Understanding the future SST changes can help practitioners better plan their activities. To evaluate the robustness and reliability of the OTCFM method across different time scales, this paper conducts a detailed comparison with four other models. We selected RMSE and MAE as evaluation metrics. We conducted repeated experiments on datasets from the South China and East China Sea, with prediction steps fixed at 1 day, 5 day, 9 day, and 14 day. Figure 2 illustrates the prediction accuracy for different steps in the datasets from the East China Sea and the South China Sea. The following conclusions can be drawn from observing Figure 2:

(1) Observing Fig. 2, it can be seen that at 1 day, the evaluation indexes of the five models reach the optimal results, among which the MAE of OTCFM is 0.285, lower than the other models. With the help of intra-period and inter-period features, OTCFM outperforms the different models in predicting the South and East China Seas datasets, with an MAE of 0.711 at 14 day, much lower than that of the LSTM of 0.990. Thanks to the assistance of the intra-period and inter-period features, OTCFM demonstrates excellent performance in predicting the South and East China Seas datasets. In particular, its MAE value of 0.711 for the 14 day prediction is significantly lower than that of 0.990 for the LSTM model. Time series data usually harbor intrinsic volatility, such as seasonal and cyclical variations. Traditionally, ConvLSTM models have effectively captured and exploited these volatilities in short-term forecasting tasks. However, in long-term forecasting, this capturing ability is limited by the uncertainty of future fluctuations, which affects the accuracy of the forecast.

(2) The challenge of forecasting increases as the forecasting period lengthens. In this regard, the OTCFM model demonstrates a better ability to fit the spatio-temporal evolutionary pattern of SST, and its performance reaches the highest level in terms of both evaluation metrics, with an MAE of 0.728. In contrast, the prediction accuracy of the ConvLSTM and TCN models is more average, with an MAE of 0.819 and 0.879, respectively, and the LSTM model is the most unsatisfactory, with an MAE as high as 0.914. The OTCFM model consistently maintains the lowest MAE and RMSE values in the SST prediction task, proving its adaptability in oceanic regions' medium- and long-term forecasting tasks. On the other hand, TCN models tend to require more computational resources for long-term forecasting. Limited by computational resources, the model's

TABLE 2. Ablation experiments of feature extraction components.

Metric	Method	South China Sea				East China Sea			
		1	5	9	14	1	5	9	14
RMSE	$(OTCFM-\hat{T}_{in})$	0.377	0.398	0.426	0.527	0.419	0.497	0.572	0.671
	$(OTCFM-\hat{T}_{Between})$	0.396	0.436	0.527	0.638	0.488	0.537	0.621	0.716
	OTCFM	0.221	0.261	0.302	0.386	0.311	0.324	0.335	0.341
R2	$(OTCFM-\hat{T}_{in})$	0.954	0.948	0.937	0.911	0.977	0.965	0.951	0.931
	$(OTCFM-\hat{T}_{Between})$	0.945	0.922	0.918	0.902	0.968	0.961	0.947	0.928
	OTCFM	0.991	0.982	0.979	0.961	0.986	0.977	0.969	0.958
MAE	$(OTCFM-\hat{T}_{in})$	0.371	0.392	0.421	0.437	0.428	0.439	0.478	0.502
	$(OTCFM-\hat{T}_{Between})$	0.389	0.402	0.444	0.451	0.476	0.491	0.505	0.518
	OTCFM	0.291	0.305	0.311	0.327	0.318	0.326	0.334	0.351
MAPE	$(OTCFM-\hat{T}_{in})$	0.83%	0.88%	0.91%	0.99%	0.89%	0.94%	1.05%	1.12%
	$(OTCFM-\hat{T}_{Between})$	0.89%	0.91%	1.01%	1.02%	0.92%	0.97%	1.08%	1.13%
	OTCFM	0.75%	0.81%	0.88%	0.94%	0.81%	0.87%	0.97%	1.04%

complexity and resolution may not adequately capture the delicate patterns in the data, which may affect the accuracy of the medium- and long-term forecasts.

C. ABLATION EXPERIMENTS OF FEATURE EXTRACTION COMPONENTS (RQ3)

To investigate the effectiveness of the intra-periodic and inter-periodic features we extracted, we will conduct three sets of variant experiments in this section to demonstrate that all these features positively impact the accuracy of SST time-series predictions. The component $x \in \{\hat{T}_{in}, \hat{T}_{Between}\}$ is provided, where $\hat{T}_{in}$ and $\hat{T}_{Between}$ represents intra-periodic and periodic features, respectively. Two ablation variant experiments were conducted based on the South China Sea and East China Sea datasets, indicating the control group experiments without embedding the corresponding components. The experimental results are shown in Table 2, where the prediction steps are set to 1 day, 5 day, 6 day, and 14 day.

As shown in Table 2, in the East China Sea SST dataset, the RMSE and MAE are 0.377 and 0.371 when the intra-periodic features are missing. In contrast, they are 0.396 and 0.389 when the inter-periodic features are missing. Thus, it can be found that the inter-periodic features play an essential role in the SST prediction task. In contrast, intra-periodic features perform poorly when used alone for SST prediction. One potential reason is that the convolutional kernel in the inter-periodic feature extraction module has some intra-periodic feature extraction capability.

Nevertheless, the feature extraction effect is insignificant in the face of the complex and variable sea area dataset. In contrast, the cross-period feature extraction module of the OTCFM model makes up for the lack of prediction performance. Combining these two modules can effectively realize medium- and long-term prediction.

D. ANALYSIS OF VISUALIZATION RESULTS FOR SEA SURFACE TEMPERATURE PREDICTION MODELS (RQ4)

Experimental Description. To intuitively demonstrate the model's prediction performance, this paper visualizes the SST forecast results from June 1, 2023, to June 7, 2023. During this period, the ENSO cycle ultimately transitioned to an El Niño state, significantly impacting sea surface temperature and making SST predictions more challenging.

Visualization Results in the South China Sea. Figure 3 presents the spatial distribution of RMSE for long-term predictions of SST in the South China Sea test set using LSTM, TCN, ConvLSTM, 3D U-Net, and OTCFM models. In the figure, darker blue indicates more minor prediction errors, while darker red indicates more significant ones.

Figure 3 shows the entire SST plot, divided into 35 subplots. Each column represents the error values of different modes in the current prediction step. Each subplot consists of 24 × 24 grids representing the prediction performance of each algorithm at various latitudes and longitudes. It can be seen that the five modeling methods have the most significant prediction errors at almost the exact locations, which may be since SST exhibits non-stationarity at these locations, resulting in changes in the spatial distribution pattern, while the LSTM and 3D U-Net are most affected in the LSTM and 3D U-Net, with more light-colored regions.

Due to the relatively stable temperature evolution process in the South China Sea, the RMSEs of the prediction results at most grid points are near 0, indicating that the prediction errors are minor. The RMSE values of all models gradually increase with the increase of the forecast step. Among them, the light-colored area in the TCN prediction results decreases, indicating that the error of TCN rises the fastest, which is strongly influenced by the cycle length. The complexity of the geophysical system leads to the challenging

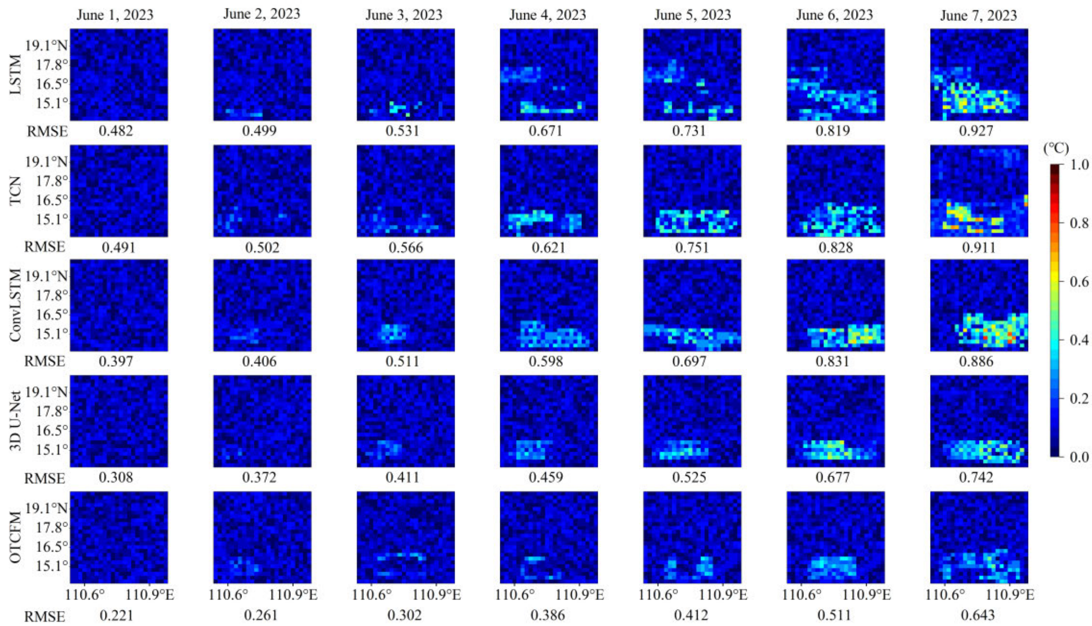

FIGURE 3. Comparison of daily RMSE errors of different models for medium and long-term forecasts in the East China Sea from June 1, 2023, to June 7, 2023.

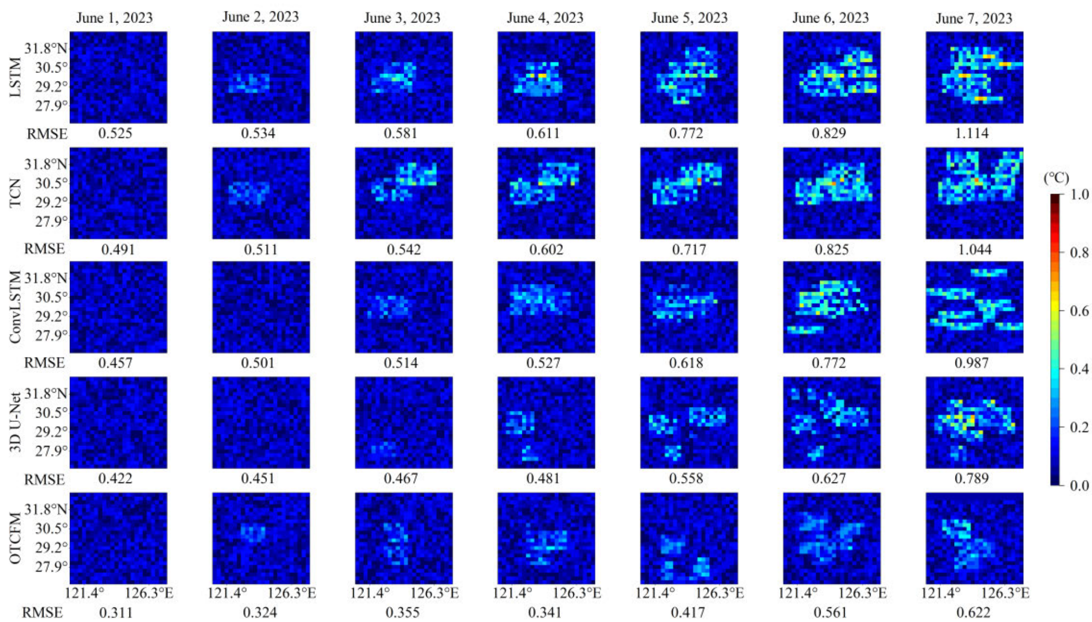

FIGURE 4. Comparison of daily RMSE errors of different models for medium and long-term forecasts in the South China Sea from June 1, 2023, to June 7, 2023.

prediction of the SST evolution pattern, and the previous methods do not consider capturing the changes in the spatial distribution pattern of SST data over different periods. The OTCFM proposed in this paper provides a new definition of the period, which can effectively capture the interactions between periods and the distribution law characteristics in different periods and improves the accuracy of the long-term prediction of SST. On 7 day, the RMSE value of the 3D U-Net is 0.742, while the RMSE value of the OTCFM model is 0.643, with almost no red zone, which is 13.3% higher than 3D U-Net.

Visualization Results in the East China Sea. Figure 4 shows the RMSE spatial distribution visualization of long-term and medium-term predictions on the East China Sea SST test set using LSTM, TCN, ConvLSTM, 3D U-Net, and OTCFM models.

By observing Figures 3 and 4, we find that the prediction performance of all models is better in the South China Sea than in the East China Sea. However, the OTCFM method performs well in both sea areas, adapting well to different prediction scenarios.

V. CONCLUSION

In this paper, we proposed a novel deep learning method named OTCFM, in which the Ocean Unit uses a residual connection approach to achieve SST prediction. The article first introduces a strategy for dividing the SST time series into periods. Then, it presents the feature extraction modules within and between periods and the adaptive fusion module, describing the entire SST prediction process in detail. We conducted repeated experiments on actual datasets and comprehensively compared OTCFM with other models. The experimental results indicate that OTCFM performs well in SST prediction tasks, particularly excelling in medium- to long-term SST forecasting compared to existing methods. Additionally, we visualized the experimental results, providing insights and guidance for future research in SST prediction tasks.

In future work, we plan to incorporate multiple oceanic factors (such as precipitation, sea level, etc.) to assist in predicting SST. Considering the complex physical environment of the Earth system, we will explore the combination of traditional physical equations and advanced deep learning techniques to gain a more comprehensive understanding and prediction of SST variations within the Earth system, thereby enhancing the ability to respond to climate change.

REFERENCES

[1] C. Zha, W. Min, Q. Han, X. Xiong, Q. Wang, and Q. Liu, "Multiple granularity spatiotemporal network for sea surface temperature prediction," *IEEE Geosci. Remote Sens. Lett.*, vol. 19, pp. 1–5, 2022.

[2] Y. Sun, X. Yao, X. Bi, X. Huang, X. Zhao, and B. Qiao, "Time-series graph network for sea surface temperature prediction," *Big Data Res.*, vol. 25, Jul. 2021, Art. no. 100237.

[3] R. Noori, M. R. Abbasi, J. F. Adamowski, and M. Dehghani, "A simple mathematical model to predict sea surface temperature over the northwest Indian ocean," *Estuarine, Coastal Shelf Sci.*, vol. 197, pp. 236–243, Oct. 2017.

[4] I. Richter, P. Chang, and X. Liu, "Impact of systematic GCM errors on prediction skill as estimated by linear inverse modeling," *J. Climate*, vol. 33, no. 23, pp. 10073–10095, Dec. 2020.

[5] E. Yati and S. Minobe, "Sea surface temperature predictability in the north Pacific from multi-model seasonal forecast," *J. Oceanogr.*, vol. 14, no. 3, pp. 25–30, 2021.

[6] I. D. Lins, M. Araujo, M. D. C. Moura, M. A. Silva, and E. L. Droguett, "Prediction of sea surface temperature in the tropical Atlantic by support vector machines," *Comput. Statist. Data Anal.*, vol. 61, pp. 187–198, May 2013.

[7] L. Wei, L. Guan, and L. Qu, "Prediction of sea surface temperature in the South China Sea by artificial neural networks," *IEEE Geosci. Remote Sens. Lett.*, vol. 17, no. 4, pp. 558–562, Apr. 2020.

[8] S. V. Kumar and L. Vanajakshi, "Short-term traffic flow prediction using seasonal ARIMA model with limited input data," *Eur. Transp. Res. Rev.*, vol. 7, no. 3, pp. 1–9, Sep. 2015.

[9] X. Shi, Z. Chen, H. Wang, D.-Y. Yeung, W.-K. Wong, and W.-C. Woo, "Convolutional LSTM network: A machine learning approach for precipitation nowcasting," in *Proc. Adv. Neural Inf. Process. Syst.*, vol. 28, 2015, pp. 1–9.

[10] S. Hou, W. Li, T. Liu, S. Zhou, J. Guan, R. Qin, and Z. Wang, "D2CL: A dense dilated convolutional LSTM model for sea surface temperature prediction," *IEEE J. Sel. Topics Appl. Earth Observ. Remote Sens.*, vol. 14, pp. 12514–12523, 2021.

[11] D. He, Q. Shi, X. Liu, Y. Zhong, G. Xia, and L. Zhang, "Generating annual high resolution land cover products for 28 metropolises in China based on a deep super-resolution mapping network using Landsat imagery," *GIScience Remote Sens.*, vol. 59, no. 1, pp. 2036–2067, Dec. 2022.

[12] Q. Shi, M. Liu, A. Marinoni, and X. Liu, "UGS-1m: Fine-grained urban green space mapping of 31 major cities in China based on the deep learning framework," *Earth Syst. Sci. Data*, vol. 15, no. 2, pp. 555–577, Feb. 2023.

[13] B. Li, B. Tang, L. Deng, and M. Zhao, "Self-attention ConvLSTM and its application in RUL prediction of rolling bearings," *IEEE Trans. Instrum. Meas.*, vol. 70, pp. 1–11, 2021.

[14] M. Han, Y. Feng, X. Zhao, C. Sun, F. Hong, and C. Liu, "A convolutional neural network using surface data to predict subsurface temperatures in the Pacific Ocean," *IEEE Access*, vol. 7, pp. 172816–172829, 2019.

[15] B. Qiao, Z. Wu, Z. Tang, and G. Wu, "Sea surface temperature prediction approach based on 3D CNN and LSTM with attention mechanism," in *Proc. 23rd Int. Conf. Adv. Commun. Technol. (ICACT)*, Feb. 2021, pp. 342–347.

[16] J. Liu, T. Zhang, Y. Gou, X. Wang, B. Li, and W. Guan, "Convolutional LSTM networks for seawater temperature prediction," in *Proc. IEEE Int. Conf. Signal, Inf. Data Process. (ICSIDP)*, Chongqing, China, Dec. 2019, pp. 1–5.

[17] Q. Zhang, H. Wang, J. Dong, G. Zhong, and X. Sun, "Prediction of sea surface temperature using long short-term memory," *IEEE Geosci. Remote Sens. Lett.*, vol. 14, no. 10, pp. 1745–1749, Oct. 2017.

[18] Z. Lin, M. Li, Z. Zheng, Y. Cheng, and C. Yuan, "Self-attention ConvLSTM for spatiotemporal prediction," in *Proc. AAAI Conf. Artif. Intell.*, Apr. 2020, vol. 34, no. 7, pp. 11531–11538.

[19] G. Zhu, L. Zhang, L. Yang, L. Mei, S. A. A. Shah, M. Bennamoun, and P. Shen, "Redundancy and attention in convolutional LSTM for gesture recognition," *IEEE Trans. Neural Netw. Learn. Syst.*, vol. 31, no. 4, pp. 1323–1335, Apr. 2020.

[20] S. Hochreiter and J. Schmidhuber, "Long short-term memory," *Neural Comput.*, vol. 9, no. 8, pp. 1735–1780, Nov. 1997, doi: 10.1162/neco.1997.9.8.1735.

[21] S. Bai, J. Zico Kolter, and V. Koltun, "An empirical evaluation of generic convolutional and recurrent networks for sequence modeling," 2018, *arXiv:1803.01271*.

[22] X. Shi, Z. Chen, H. Wang, D. Y. Yeung, W. K. Wong, and W. C. Woo, *Convolutional LSTM Network: A Machine Learning Approach for Precipitation Nowcasting*. Cambridge, MA, USA: MIT Press, 2015.

[23] B. Xie, J. Qi, S. Yang, G. Sun, Z. Feng, B. Yin, and W. Wang, "Sea surface temperature and marine heat wave predictions in the South China Sea: A 3D U-Net deep learning model integrating multi-source data," *Atmosphere*, vol. 15, no. 1, p. 86, Jan. 2024, doi: 10.3390/atmos15010086.

[24] M. Zhang, G. Han, X. Wu, C. Li, Q. Shao, W. Li, L. Cao, X. Wang, W. Dong, and Z. Ji, "SST forecast skills based on hybrid deep learning models: With applications to the South China Sea," *Remote Sens.*, vol. 16, no. 6, p. 1034, Mar. 2024, doi: 10.3390/rs16061034.

LU-YI FAN is currently pursuing the bachelor's degree with the Business School, Hohai University, Nanjing, China. His research interests include machine learning and data mining.

YU-HAO CAO is currently pursuing the bachelor's degree with the School of Computer Science and Technology, Wuhan University of Science and Technology, Wuhan, China. His research interests include machine learning and machine vision.

NING-YUAN HUANG is currently pursuing the bachelor's degree with the College of Computer and Information Engineering (College of Artificial Intelligence), Nanjing Tech University, Nanjing, China. His research interests include computer vision, deep learning, and embedded development.

GUO-XUAN SUN is currently pursuing the bachelor's degree with the Business School, Hohai University, Nanjing, China. His main research interests are machine learning and data mining.

JIA-NING CAO is currently pursuing the bachelor's degree with the Business School, Hohai University, Nanjing, China.

CHANG-XU LIU is currently pursuing the bachelor's degree with the College of Computer and Information Engineering (College of Artificial Intelligence), Nanjing Tech University, Nanjing, China. His research interests include deep learning, computer vision, and computer networks.